8-8-2013

An Assessment of worldview-2 imagery for the classification of a mixed deciduous forest

Nahid Carter

An Assessment of Worldview-2 Imagery for the Classification Of a Mixed Deciduous Forest

by:

Nahid Carter

Rochester Institute of Technology

College of Science: Thomas H. Gosnell School of Life Sciences

Program of Environmental Science

A thesis submitted in partial fulfillment
of the requirement for the degree
of Master of Science

Approved

August 8, 2013

by:

_____
Elizabeth N. Hane, Ph.D.
Chair of Committee

_____
Karl F. Korfmacher, Ph.D.

_____
Jan van Aardt, Ph.D.

Abstract

Remote sensing provides a variety of methods for classifying forest communities and can be a valuable tool for the impact assessment of invasive species. The emerald ash borer (*Agrilus planipennis*) infestation of ash trees (*Fraxinus*) in the United States has resulted in the mortality of large stands of ash throughout the Northeast. This study assessed the suitability of multi-temporal Worldview-2 multispectral satellite imagery for classifying a mixed deciduous forest in Upstate New York. Training sites were collected using a Global Positioning System (GPS) receiver, with each training site consisting of a single tree of a corresponding class. Six classes were collected; Ash, Maple, Oak, Beech, Evergreen, and Other. Three different classifications were investigated on four data sets. A six class classification (6C), a two class classification consisting of ash and all other classes combined (2C), and a merging of the ash and maple classes for a five class classification (5C). The four data sets included Worldview-2 multispectral data collection from June 2010 (J-WV2) and September 2010 (S-WV2), a layer stacked data set using J-WV2 and S-WV2 (LS-WV2), and a reduced data set (RD-WV2). RD-WV2 was created using a statistical analysis of the processed and unprocessed imagery. Statistical analysis was used to reduce the dimensionality of the data and identify key bands to create a fourth data set (RD-WV2). Overall accuracy varied considerably depending upon the classification type, but results indicated that ash was confused with maple in a majority of the classifications. Ash was most accurately identified using the 2C classification and RD-WV2 data set (81.48%). A combination of the ash and maple classes yielded an accuracy of 89.41%. Future work should focus on separating the ash and maple classifiers by using data sources such as hyperspectral imagery, LiDAR, or extensive forest surveys.

Acknowledgements

To my committee members, Elizabeth Hane, Karl Korfmacher, and Jan van Aardt, I would like to convey my deepest appreciation. It is because of your guidance and knowledge that I am the scientist that I am today. I would also like to thank the faculty and students of the Environmental Science Department for their assistance and support during my time at RIT. Also, I would like to thank my friends for providing encouragement and support.

To my parents, brother and sister, your patience, understanding and love is a perpetual source of strength. Thank you for your continued and constant support.

Table of Contents

List of Figures v
List of Tables vi
Abbreviations vii
1. Introduction 1
1.1 Overview 1
1.2 Defining Invasive Species Management 2
1.3 Emerald Ash Borer Infestation 4
1.4 Lesson from Past Invasions 5
1.5 Target Species 9
1.6 Remote Sensing 10
1.6.1 Passive Remote Sensing Data 11
1.6.2 Active Remote Sensing Data 12
1.7 The Emerald Ash Borer 13
1.8 Literature Review 18
1.9 Objectives 21
2. Methodology 22
2.1 Site Description 22
2.2 Imagery 23
2.3 Data Collection 23
2.4 Pre-classification Imagery Preparation 25
2.5 Statistical Data Reduction 26
a. 27
b. 27
c. 27
2.6 Spectral Analysis 28
2.6.1 Classification Types 28
2.6.2 Classification Procedure 28
3. Results 29

4. Discussion 31
4.1 Classification analysis 31
4.2 Multi-temporal Analysis 32
4.3 Ecological Impacts 34
5. Conclusions 36
Appendix A 39
Appendix B 41
Bibliography 50

List of Figures

Figure 1: Emerald ash borer size comparison 1
Figure 2: Map of ash distribution throughout the state of New York 8
Figure 3: Diagram of the basic operation of a multispectral sensor 11
Figure 4: Diagram of the basic concept and operation of a hyperspectral sensor 12
Figure 5: Diagram of LiDAR sensor operation 13
Figure 6: Example of LiDAR data point displayed in 3-D space 13
Figure 7: Map of the distribution of emerald ash borer infestations in the Northeastern United States 14
Figure 8: Map of emerald ash borer infestations throughout the state of New York 15
Figure 9: Example of an emerald ash borer and D-shaped exist hole 16
Figure 10: Example of vertical larval galleries as a result of emerald ash borer infestation 16
Figure 11: Example of an emerald ash borer monitoring trap 17
Figure 12: Comparison of ash and maple spectral signatures 33

List of Tables

Table 1: Worldview-2 spectral ranges for each of the eight bands 23
Table 2: Classification and ground truth points collected and corresponding class 24
Table 3: Number and type of variable derived from the June (a), September (b) and Layer Stacked data set (c) 27
Table 4: Class accuracy of ash and maple for the different data sets and classification groups ... 29

Abbreviations

EAB	Emerald Ash Borer
2C	2 Classes
5C	5 Classes
6C	6 Classes
J-WV2	June Worldview-2
S-WV2	September Worldview-2
LS-WV2	Layer Stack Worldview-2
RD-WV2	Reduced Data Worldview-2

1. Introduction

1.1 Overview

Invasive species pose a serious threat to environmental conservation and biodiversity on a worldwide scale. The impact that these invaders have on both native ecosystems and economic infrastructures is of concern, as the list of invasive species continues to grow. In the United States alone there are an estimated 50,000 non-native species that have led to an environmental damage estimate of $120 billion per year in economic losses (Pimentel *et al*. 2005). Among the invasive species in North America, the *Agrilus planipennis*, also known as the emerald ash borer (EAB), has received particular attention. The EAB is a green, wood-boring beetle from Asia that infests members of the *Fraxinus* genus (Figure 1). It is estimated to have caused the death of 53 million ash trees since accidental introduction in 2005 (Kovacs *et al*. 2010).

Figure 1: An Emerald Ash Borer on top of a penny for size comparison (*Photo: Howard Russell, MI State U., www.forestryimages.org*.)

The threat of invasive species has prompted various methods of detection and management. An increasingly popular method for invasive species detection is remote sensing, which can provide accurate, reliable, and large scale recognition. Used in time-series format, remote sensing analyses can be used to detect, track and monitor invasive species, infestations, and spread.

1.2 Defining Invasive Species Management

The continued spread of existing invasive species, as well as the introduction of new species, has prompted some ecologists to question the accepted paradigm concerning invasive species management. Two schools of thought have developed upon this subject. The first asserts that constant vigilance and the implementation of precautionary measures are necessary, in order to block or reduce the spread of non-native species. The second is that not all introduced species are malicious, and that it is nearly impossible to monitor and track them all. Hence, it is better to concentrate eradication and control efforts on a few that have serious ecological or economic impact.

Formatted: Condensed by 0.2 pt

Ruesink *et al* (1995) suggested that all foreign species be treated as dangerous until proven otherwise in terms of potential harm, and supported this statement with three case studies. The first is the decision to not introduce channel catfish (*Letalurus punctatus*) into New Zealand. By basing the decision on damage done by previous introductions in other environments and the likelihood of escape, it was decided to not go through with the introduction, avoiding potential ecological and economic damage.

The second case study involved the study of a family of shrubs and trees, *Banksia*, a native of Western Australia, but imported and cultivated in Africa. Richardson *et al* (1990) used life-history characteristics to predict which species of *Banksia* may invade the fynbos, a rare, extremely biodiverse, fire-dependent ecosystem. The authors looked at pine species that had successfully invaded the fynbos, and determined that key life-history characteristics shared by the species were small seeds with large wings, short juvenile periods, serotinous cones, and adults that were killed by fire. The authors then extrapolated between plant families and found 14 species within the *Banksia* genus that shared the same life-history characteristics, and therefore

were most likely to invade the fynbos. They concluded that it cannot be said with certainty that an introduced species will be a successful invasive based upon certain attributes. However, using a habitat specific approach, it is possible to identify functional groups that have a high probability of successful invasive introduction (Richardson *et al*. 1990).

In the final case study, the US Forest Service was concerned that the importation of Siberian timber into the United States might bring with it pests or diseases, and placed a ban on imports. By defining risk as the product of the probability of an infestation; assuming survival during transport, detectability, ease of establishment, spread, and likelihood of association with logs, and the magnitude of effects; economic, social, political, environmental, they determined potential pest impacts on the United States. The authors determined that there were 175 possible pests that might be introduced, of which 36 were deemed to be at a high risk for invasion and analyzed further. Based upon the model that the authors created, they estimated that the US Forest Service's decision to ban Siberian imports potentially prevented losses to the timber industry of approximately $58 billion, as well as the elimination of certain tree species, food web changes, and forest to grassland conversion. Rusink *et al* (1995) used these case studies to illustrate that the best option for preventing invasive species spread in the world is to restrict nonindigenous species entrance. The final case study is especially relevant to the EAB infestation.

Formatted: Condensed by 0.1 pt

On the other side of the argument is a growing group of ecologists that argue that the current mentality of invasive species prevention is extreme (Davis *et al*. 2011). For instance, they point to the continual failure since 1996 to eradicate invasive plants in the Galapagos. Even though there have been 39 attempts, only four have been successful. Also, they point to the devil's claw plant (*Martynia annua*) and tamarisk shrubs (*Tamarix* spp.) as species that garner

considerable negative attention from both the government and the public, yet there is little evidence to show any harm to the environment. They propose that instead of automatically categorizing a foreign species as invasive, and therefore subject to management or eradication, scientific evidence should be used to determine the impact a species has on an ecosystem. If an exotic species does not cause human health or economic harm, then it should not be considered an invasive species. The authors do not dismiss the impacts that invasive species can have on the environment. Invasive species, such as zebra mussels, and avian malaria, have driven extinctions and damaged environmental services. Avian malaria has resulted in the extinction of more than half of Hawaii's native birds species and zebra mussels have cost the US power and water utilities hundreds of millions of dollars in damage from clogged pipes. Davis *et al* (2011) state that while invasive species have had negative impacts on the environment, the majority of introduced species cause minimal, if any, harm to the ecosystems they invade.

1.3 Emerald Ash Borer Infestation

In the context of this controversy, the infestation by the EAB of the northeastern United States ash population poses an interesting ecological question: should the EAB be considered an invasive species and therefore be controlled or eradicated? The approach that Ruesink *et al* (1995) would recommend is to contain and control the current EAB infestation and to take precautions to limit the continued spread. Initiatives such as the banning of camp fire wood transport between counties and states, as well as insecticide injections into to uninfested ash trees, are already being pursued. For example, EAB was found in the City of Rochester, in New York, in June of 2010 (Schubert 2010). Prior to the EAB being discovered, the City of Rochester Forestry Division had conducted an inventory of all trees that fall under the City's jurisdiction. It

was estimated that 5,000 ash trees, 8% of the total inventory, exist within the city limits. While it is possible to remove all the ash trees at once, a procedure that would leave some streets totally bare of tree cover, the city chose a less disruptive route. All visibly unhealthy and infested trees were removed immediately, while remaining trees were treated with TREE-age, an insecticide that is injected directly into the trunk and is expected to prevent infestation for two to three years. Once the treatment period is over, trees will either be retreated or removed. Where ash has already been removed, different species have been planted to replace it, allowing for a gradual urban forest transition.

While the foreign origins of the EAB would automatically categorize it as an invasive species according to Ruesink *et al* (1995), Davis *et al* (2011) may categorize it an invasive for different reasons. As stated earlier, Davis *et al* (2011) identify an invasive species by its economic and human health impact. A growing body of evidence supports the EAB being considered an invasive. Spread scenarios estimate the mortality of 700 million ash trees in Michigan alone (Herms *et al*. 2004). Kovacs *et al* (2010) estimated the possible cost of treatment, replacement, and removal of ash trees on developed land as a result of EAB infestation over a 10 year period at $10.7 billion.

1.4 Lesson from Past Invasions

The EAB is not the first potentially serious threat to the North American forest ecosystems. Ellison *et al* (2005) used the following description of a foundation species: “a single species that defines much of the structure of a community by creating locally stable conditions for other species, and by modulating and stabilizing fundamental ecosystem processes.” Examples of lost North American foundation species resulting in significant impacts on their

respective environments include American chestnut (*Castanea dentate*) and Eastern hemlock (*Tsuga canadensis*). Both of these species played key roles in nutrient cycling and habitat creation in their respective ecosystems.

The American chestnut constituted a significant proportion of northeast forest communities, along with oak, and exerted a heavy influence on the environment. Chestnut blight, which resulted from the accidental introduction of the canker pathogen, *Cryphonectria parasitica*, from Asia, decimated the chestnut population within 50 years of introduction (Ellison *et al*. 2005). Presently, chestnut exists as an understory shrub with very few fully grown, mature trees left. Chestnuts are thought to have had far-reaching impacts on the ecosystem structure of the forest communities where they lived, and that their removal has changed the forests irreparably. There is evidence that chestnut produced allelo-chemicals that suppressed the growth of eastern hemlock and rhododendron along riparian corridors, species that are currently thought of as common for that type of environment (Ellison *et al*. 2005). Additionally, chestnuts rapid growth and sequestration of carbon and nutrients, low C:N ratio, and high tannin content would have had strong influences on decomposition, productivity, and nutrient cycling. Chestnut is a quickly decomposing and highly nutritional food source to forest stream systems. The change from chestnut to oak, a much more slowly decomposing and lower nutritional food source, would have resulted in decreased growth rates and body size of aquatic macroinvertebrates (Ellison *et al*. 2005).

The loss of the Eastern hemlock due to the hemlock woolly adelgid (*Lambdina fiscellaria*) resulted in changes to the ecosystem, because of a similar decline as the American chestnut. Hemlock stands create unique microclimates that are cool, damp, and have very slow

nitrogen-cycling within nutrient poor soil (Ellison *et al*. 2005). Furthermore, hemlock canopy transpiration and snow-interception rates decrease stream temperature profile variation and stabilize soil moisture and stream base flows, supporting distinctive assemblages of salamanders, fish, and freshwater invertebrates (Ellison *et al*. 2005). Unlike the American chestnut, which can be found growing in the understory as a shrub, the Eastern hemlock typically does not re-establish after a woolly adelgid invasion. Instead, hemlock range lost to adelgid mortality is being colonized by birch (*Betula* spp.), oak (*Quercus* spp.), maple (*Acer* spp.), and yellow poplar (*Liriodendron tulipifera*) (Ellison *et al*. 2005). The loss of the Eastern hemlock would alter stream ecosystems, cause the loss of uniquely associated plants and birds, and impact nutrient and hydrological cycles.

The American chestnut and Eastern hemlock illustrate the ecological impact that the loss of a foundation species can have on an ecosystem. The widespread infestation and mortality of ash by the EAB, is similar to that of the American chestnut and Eastern hemlock in both scope and possible severity. Ash represents a large portion of forest cover in Monroe County and New York State (Figure 2). While the importance of ash in the local forest community is not fully known, species richness is relatively low. Considering that there are only a few tree species, including ash, that account for most of the cover in the forest community, loss of ash will have some impact on the ecosystem. The severity of the impact, however, is unknown.

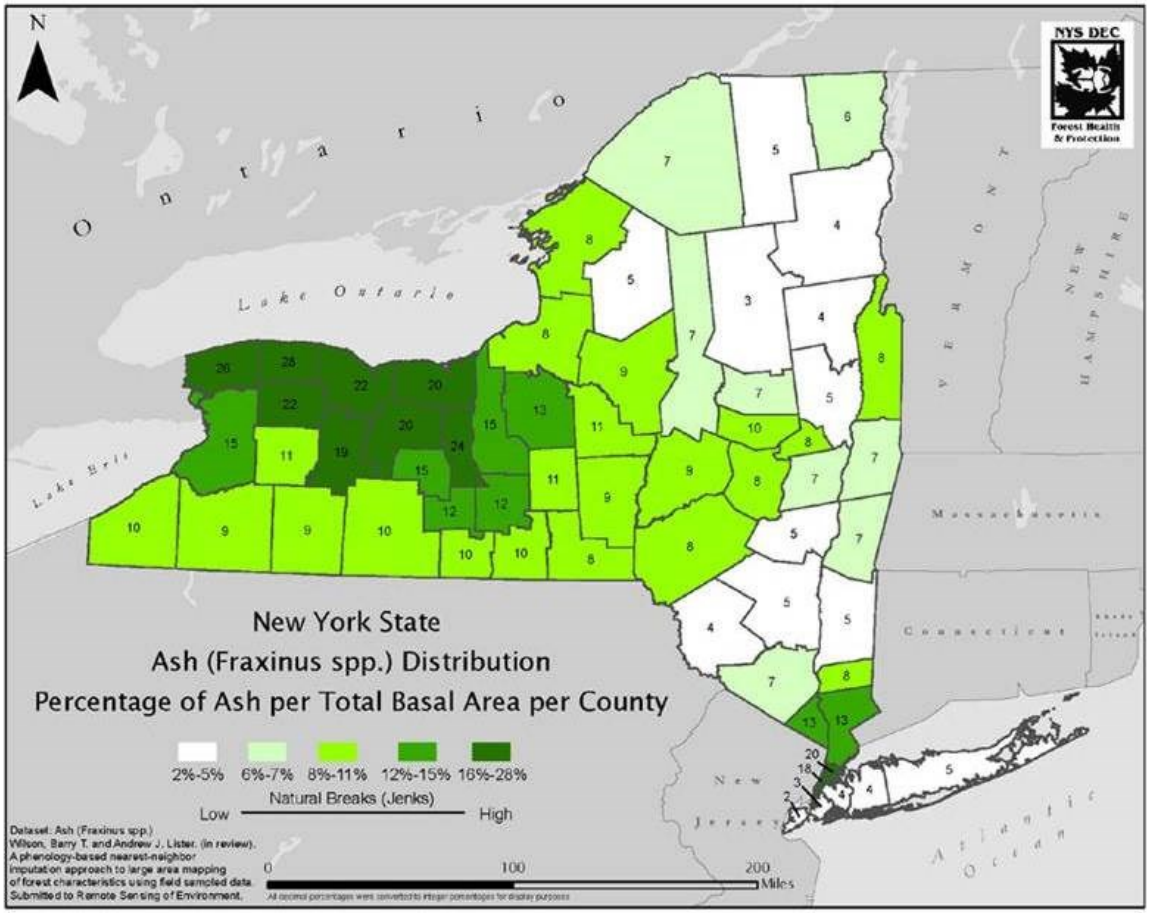

Figure 2: Map of the percentage of ash per total basal area per county. Monroe County falls in the 16%-28% range.

1.5 Target Species

Fraxinus is a large tree genus that has member species worldwide. In the Great Lakes region, the ash species present are white ash (*Fraxinus americana*), green ash (*Fraxinus pennsylvanica*), black ash (*Fraxinus nigra*), and to a lesser extent blue ash (*Fraxinus quadrangulata*) and pumpkin ash (*Fraxinus profunda*). The ash genus is characterized by opposite feather-compound leaves and canoe shaped winged fruit (Petrides and Wehr, 1998). Ash is an important component of both urban and natural woodlands. They are common street trees in urban areas (Kashian and Witter, 2011) as well as being an important timber species for furniture, baseball bats, and tool handles. Ash grow in a number of different ecosystems ranging from upland dry areas (white ash) to poorly drained swamp areas (black ash) and seasonally saturated environments (green ash) (Kashian and Witter, 2011). White ash is a dominant species in forest ecosystems, primarily in Michigan and northwestern Wisconsin, where it is considered an indicator species of certain habitat types in upper Michigan and northwestern Wisconsin (Griffith, 1991). White ash is a source of browse for deer, wood duck, northern bobwhite, purple finch, fox squirrel and other birds and mammals. It readily provides trunk cavities that provide key nesting for a number of woodpecker species, wood duck, grey squirrels, and owls (Griffith, 1991). It is unclear what the impact of the loss of this species will be on the multiple ecosystems that the ash genus inhabits. It has been demonstrated both experimentally and in the field that EAB readily parasitize all four species (Anulewicz *et al*. 2008).

1.6 Remote Sensing

Campbell and Wynne (2011) defined the overall field of remote sensing as the observation of an object from a distance without physically contacting it. In general, remote sensing falls into one of two types of collection methods, passive and active.

Passive remote sensing relies upon recording the energy reflected or emitted by an object. In their book, Introduction to Remote Sensing , Campbell and Wynne (2011) divide passive remote sensing into two categories; the first being the recording of solar radiation reflection off a surface, the second being the recording of the radiation emitted by an object. There is an important distinction between recording either the energy reflected or emitted by an object. An example of a passively recording reflectance is photography, or orthoimagery, discussed later (Campbell and Wynne, 2011).

The other passive category differs from the first in that it records emitted energy in the far infrared, or other wavelength, not visible to the naked eye. This can be further divided into multispectral and hyperspectral imagery collect, which will be discussed later. These types of imagery can be used, for example, to assess chlorophyll status in plants, evaluate leaf area index, and estimate plant stress based upon the recording of emitted energy at certain wavelengths (Horler *et al*. 1983). **Active remote sensing** uses an energy source and records the reflection of that energy off of an object. Campbell and Wynne (2011) provide an example of an active remote sensing system is a camera with a flash attachment.

1.6.1 Passive Remote Sensing Data

Passive remote sensing can be divided to three types of imagery; orthoimagery, multispectral imagery, and hyperspectral imagery. Orthoimagery is a traditional color or panchromatic image of the target area, georectified to remove camera distortions at the edge of the photo and orthorectified to display objects without tilt and in the proper location. Multispectral imagery consists of a sensor collecting light reflected by an object into specified groups, or bands, such as 400-450nm (Figure 3). Finally, hyperspectral imagery is similar to multispectral imagery in that it represents reflectance but instead of large frequency ranges generalized to a few bands, it usually has very narrow frequency ranges and many contiguous bands (Figure 4). Passive remote sensing is used in a number of different fields, and its ability to analyze large areas with minimal field surveys has seen a growing use in the detection and tracking of invasive species.

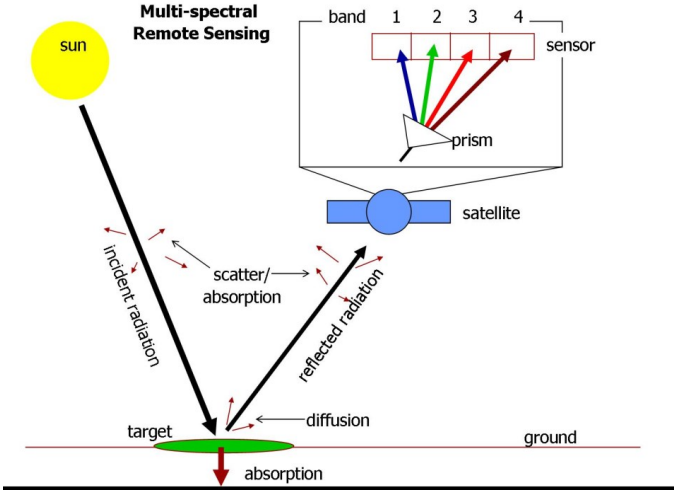

Figure 3: The diagram shows the basic operation of a multi-spectral device. Light energy is reflected off an object and a sensor collects this energy and distributes it into different bands that have a set wavelength collection range (wr.udel.edu).

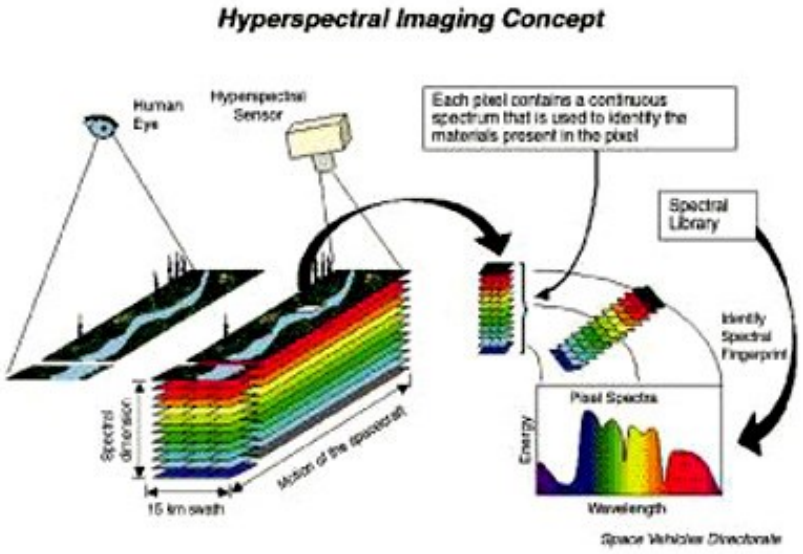

Figure 4: The diagram shows the concept and operation of a hyper-spectral device. Light energy is reflected off an object and is collected by sensor. Different object reflect light at a different spectrum and this energy is categorized into many narrows wavelength ranges (st.gsfc.nasa.gov).

1.6.2 Active Remote Sensing Data

LiDAR is a remote sensing system that has found uses in a wide array of disciplines including forestry, geography, military applications, mapping, meteorology, and other scientific and commercial fields. The basic design of a LiDAR system consists of a laser that pulses a specified number of times a second, for instance 200kHz. Combined with the laser is a sensor to detect the returning laser pulse after it hits an object and bounces back. A return time is recorded with each returning laser pulse and this return time can be translated into a distance from the source (Figure 5). These distances can then be converted into a 3D point cloud of a target, such as a forest canopy (Figure 6). By assessing the 3D structure of individual trees or forest canopies,

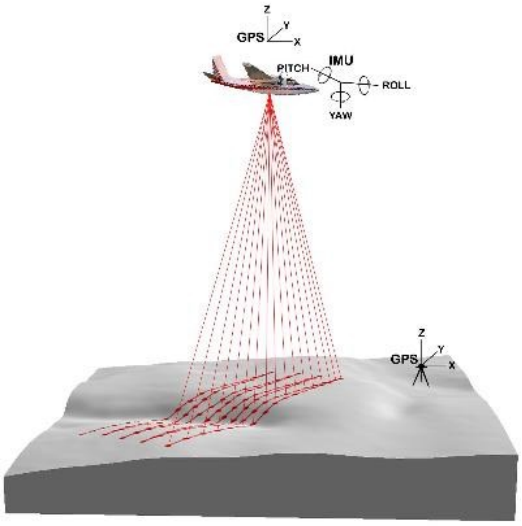

Figure 5: This diagram shows the operation of an airbourne LiDAR system. As the plane flies over a landscape laser pulse returns are recorded based upon the time the pulse was emitted and the time for that pulse to return to the sensor (USDA Forest Service).

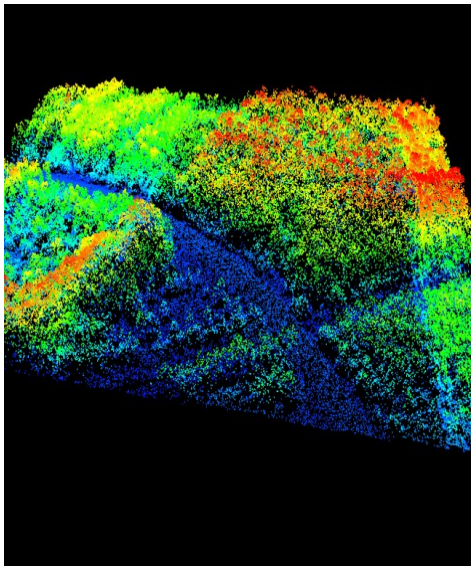

Figure 6: A LiDAR image of a forest area on the Rochester Institute of Technology campus. The blue dots represent lower elevations, such as a road, and the red dots represent the highest elevations, the tops of the forest canopy.

it is possible to estimate forest biomass using specific algorithms. Physical characteristics such as diameter at breast height (DBH), and height are important variables in biomass and carbon sequestration equations. Structural data that can be collected using LiDAR systems can be used to classify forest communities as well as estimate biomass.

1.7 The Emerald Ash Borer

EAB larvae feed on the phloem, cambium, and shallow sapwood of ash trees while adults feed on leaves (Wang *et al*. 2010). Within 3-5 years, ash mortality in a healthy stand can approach 85% (Kashian and Witter 2011). In its natural environment, the EAB is reported to be able to disperse up to 1.1 km per year (Wang *et al*. 2010), however, Taylor *et al* (2010) found

that mated females may fly more than 3km or more in a single day and up to 7.2 km in four days. The distance that could potentially be covered by an EAB female in search of host trees for egg laying is well over the earlier assumptions of a half mile per year spread rate (Taylor *et al*. 2010), indicating a more rapid invasion. Figure 7 shows infestation points regionally dispersed over the northeastern United States. It is believed that the EAB was introduced via shipping crates constructed from infested timber. The extensive and rapid spread of the EAB is believed to be due to transportation of infested campfire wood, timber, and nursery stock from infested to un-

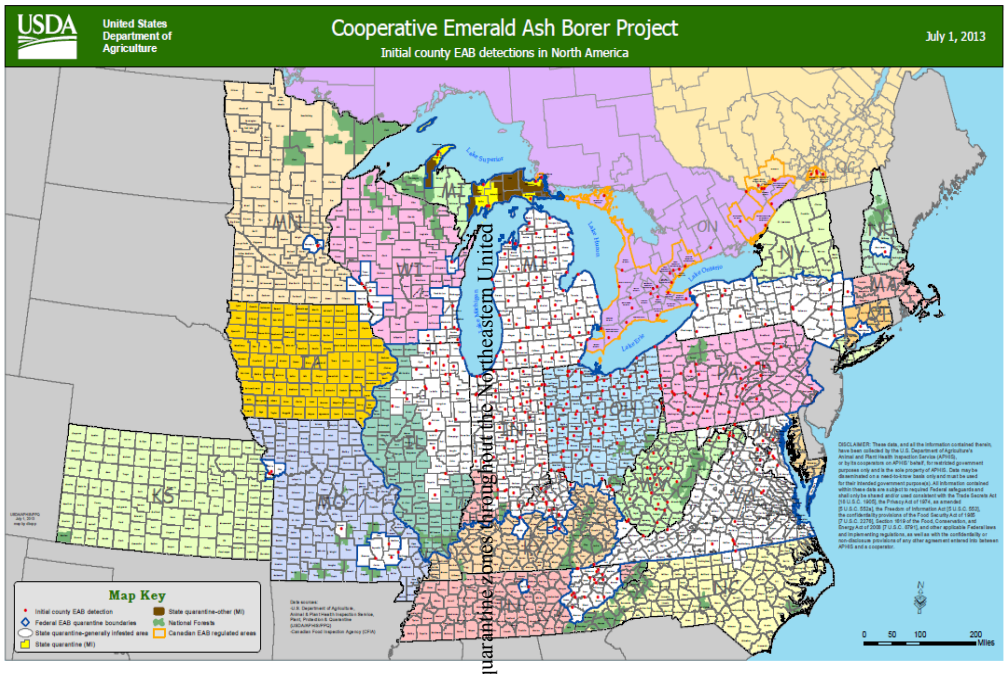

Figure 7: This figure shows the known infestation sites and quarantine zones throughout the Northeastern United States (USDA, 2013).

infested areas (Bendor *et al*. 2006).

The EAB was discovered in southeastern Michigan in June 2002 and as of 2011 has spread to 15 states and two Canadian provinces (Figure 7). Recently the EAB has been

discovered in multiple counties (Cattaraugus, Erie, Genesee, Livingston, Orange, Steuben, Greene, Ulster, and Monroe) in New York (Figure 8). Within Monroe County, the EAB infestations have been found by the New York State Department of Environmental Conservation (DEC) in the Chili-Scottsville area as well as reported sightings in Mendon and Pittsford (Schubert, 2010). Additionally, an EAB infestation was found in the Upper Falls Park in

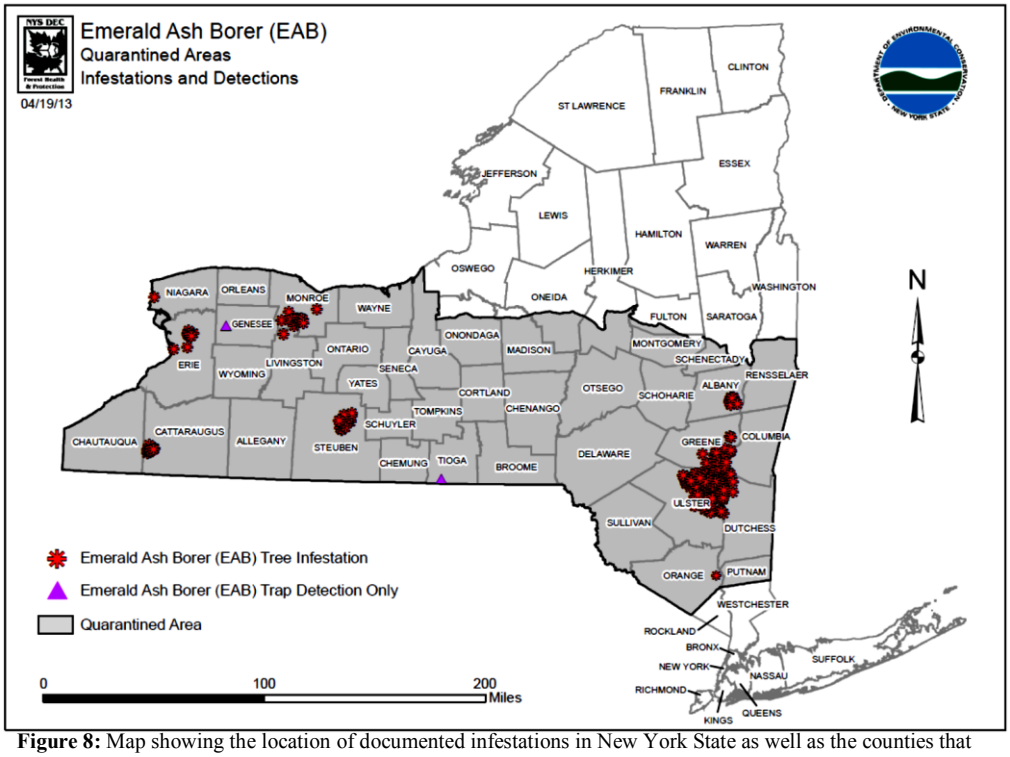

Figure 8: Map showing the location of documented infestations in New York State as well as the counties that the infestations were found in and the quarantine zones established to limit EAB spread (NYSDEC, 2013).

Downtown Rochester by forestry personnel in June 2011.

Signs of EAB infestation include D-shaped exit holes (Figure 9), canopy dieback, bark splits and peeling, epicormic shoots, and vertical larval galleries (Figure 10). These characteristics of EAB infestation make early detection difficult and therefore are only noticed

when the EAB population is high and ash trees begin dying (Wang *et al*. 2010). The threat that the EAB poses, both ecologically and economically, has prompted a number of monitoring, containment, and eradication methods to be explored. The hidden stages of the EAB lifecycle in the cambium of host ash make monitoring challenging because an infestation is only confirmed if an ash tree is already infested and dying or adult EAB are captured via traps in the area, in which case the area ash are probably already infested. EAB traps are prism shaped structures, colored purple, and coated with non-toxic glue and a lure, Manuka oil (Figure 11). If infested trees are found, the typical response is to remove them and others around them to prevent additional spread.

Figure 9: Example of a D-shaped exit hole that is characteristic of emerald ash borer (EAB) infestation. (http://www.inhs.illinois.edu/outreach/EAB.htm)

Figure 10: Example of vertical larval galleries that is an indication of emerald ash borer (EAB) infestation. (NYSDEC)

In cases where the ash trees are believed to still be healthy and removal is not desirable, insecticides are used as a preventative measure. This method involves drenching the soil around the roots of the tree with insecticide or directly injecting it into the tree trunk. A study by Mckenzie *et al* (2010) found the trunk injection chemical azadirachtin to have a strong effect

on EAB larval development in ash trees that were treated before exposure to EAB and for trees treated after EAB infestation. They found that larval development ceased after the second-instar stage, indicating that Azadirachtin was very effective for both prevention of infestation and treatment after infestation. Possible collateral damage to other non-target species, specifically decomposer invertabrates, as a result of Azadirachtin application has been researched. Kreutzweiser *et al* (2011) fed treated ash leaves to earthworms and microbial decomposers and compared the survival, leaf consumption rates, growth rate, and cocoon production to controls. There was no signification reduction in any of the comparisons, except for a reduction in microbial decomposition at the highest test concentration of Azadirachin (~6 mg kg-1).

Figure 11: Example of an emerald ash borer monitoring trap. It is purple to attach the EAB and coated with a non-toxic glue and lure, Manuka oil. (http://www.ci.roseville.mn.us/index.aspx?NID=2057)

Finally, in order to contain the spread of the EAB and also not cause potential harm to the environment, biological controls are being investigated. While an invasive species can be a serious problem outside of its home range, it is usually neutralized or controlled within its native environment. In Asia, where the EAB is native, Wang *et al* (2010) found that a parasitoid, *Spathius agrili*, was found to the major insect predator of larvae and noted the potential for biological control in the United States. In addition, Duan *et al* (2011) found that another parasitoid, *Blacha indica*, first sited in Virginia in 1995, has been found to prey upon EAB

throughout larvae, prepupae, and pupae life stages. Duan *et al* (2009) found that *B. indica*, *Eupelmus pini*, *Dolichomitus vitticrus*, and two unidentified species caused 3.6% parasitism in EAB.

Formatted: Condensed by 0.2 pt

1.8 Literature Review

Remote sensing has been widely researched as a means to classify natural communities (Miguel-Ayanz and Biging 1997, Lu *et al*. 2008, Yang and Everett 2010, Dinuls *et al*. 2012). More specifically, the multi-spectral sensor, WorldView-2, has been used for forest species classification with promising results. Abd *et al* (2012) were able to achieve species classification accuracies of 23.7% to 83.2%, depending upon the species, by collecting spectral reflectance values in the field for training. In another recent study, Immitzer *et al* (2012) achieved an overall classification accuracy of 82% with ten different species and single date imagery in a temperate forest in Austria. Worldview-2 imagery has also been used for identifying volcanic ash plumes and inferred height (McLaren *et al*. 2012).

Multiple studies have investigated the influence that multi-temporal imagery can have on classification accuracies (Ghioca-Robrecht *et al*. 2008, Townsend and Walsh 2001, Tso and Mather 1999). Hill *et al* (2010) conducted a study in Monks Wood in eastern England using five images collected throughout the growing season. Using one image, the highest overall accuracy the authors obtained was 71% (kappa 0.63). When images were combined, the overall accuracy increased to a maximum of 84% (kappa 0.79)

There are a number of other multi-spectral sensors whose utility has been assessed for forest and vegetation classifications. Lu *et al* (2008) used both Landsat Thematic Mapper (TM) and SPOT High Resolution Geometric (HRG) imagery for vegetation classifications in the

Brazilian Amazon. Overall classification accuracies ranged between 46.3% and 61.8% depending upon the data fusion method. The authors attribute this poor accuracy to the complex environment that the Amazon exhibits. This mixture results in pixel mixing and confusion. Another study used Landsat TM and SPOT HRG imagery for classifying land cover in Central Sierra Spain (Miguel-Ayanz and Biging 1997). They found that the Landsat TM imagery was able to correctly classify five of the most abundant classes, which made up 72% of the scene, to an overall accuracy of 90%. They point out that sample size may play a part in the achieving higher overall accuracies, because classes that represented a smaller proportion of the scene will have unequal total training size compared to the dominant land classes.

Formatted: Condensed by 0.1 pt

Hyperspectral sensors have also been used for land cover classifications with strong results. Yang and Everett (2010) used a hyperspectral sensor attached to a Cessna to collect imagery over an Ashe juniper site in central Texas. They also collected field reflectance values of the study site. The authors evaluated a number of supervised classification techniques including minimum distance, Mahalanobis distance, maximum likelihood, spectral angle mapper, and mixture tuned matched filtering. Overall accuracy was 93%, 91%, 91%, 87%, and 92% for the respective classifications. Because hyperspectral imagery contains such a large amount of data from very small band spectral ranges, it is possible to identify very specific wavelengths associated with target classes. This makes it possible to identify land cover or forest species much more accurately than would be possible with multispectral imagery. However, with such as large amount of data available, date reduction becomes a necessity.

Active remote sensing devices, such as LiDAR sensors, when combined with spectral imagery data, have been shown to increase classification accuracies. LiDAR has also been used

on its own for classifying land cover. Because LiDAR is able to provide forest attributes such as height, above ground biomass, and diameter at breast height, this adds additional identifying factors for forest classifications. Neuenschwander *et al* (2009) compared LiDAR data and Quickbird imagery for land cover classification accuracy on a ranch in San Marcos, Texas. Overall accuracy was 85.8% and 71.2% for the LiDAR and Quickbird imagery respectively. Another study assessed a combination approach of multispectral imagery and LiDAR data for classifying a forest in Latvia and determined that it is possible, under favorable conditions, to achieve 97% overall accuracy (Dinuls *et al*. 2012).

1.9 Objectives

The detection and management of the emerald ash borer (EAB) is a challenging task due to: 1) difficulty in predicting it's spread and; 2) once an infestation is discovered it is often too strongly established to eradicate. An important part of managing the EAB infestation is early detection and monitoring. Remote sensing can be a valuable tool for this purpose by providing broad scale assessments of given areas in order to target specific areas of interest, namely stands of ash trees. This study looked to evaluate the feasibility of 8-band multispectral Worldview-2 data to classify a mixed deciduous forest on the Rochester Institute of Technology (RIT) campus, with a focus on identifying the ash population present to a percent accuracy level of 85% or higher. The results of this research may assist management and monitoring of EAB infestations and better characterize the Worldview-2 sensor's utility for forest classifications.

Thus my goals are:

- Assess the utility of WorldView-2 imagery for genus (specifically *fraxinus*) level forest classification.
- Determine the influence of multi-temporal imagery.
- Estimate the impact the EAB will have on the forest community.

2. Methodology

2.1 Site Description

This study was conducted on the campus of the Rochester Institute of Technology (RIT) located in the Town of Henrietta in Monroe County New York (43° 5' 3.88" N, 77° 40' 29.81" W). Monroe County lies within the ecoregion described by the New York State Department of Environmental Conservation (NYSDEC) as the Great Lakes EcoRegion. The region was formed 14,000 years ago during the last Ice Age and distinguished by lake plains and low level landscapes (NYSDEC). The area receives approximately 34 inches of precipitation per year and an average 100 inches of snow fall (NYSC). The mean temperature is 47.6° Fahrenheit with extremes of 100° F to -20°F, with Lake Ontario exerting some influence on local climates (NYSC). The soil composition on the RIT campus consists of mostly Canandaigua Loam and Niagara Loam that account of an estimated 23.4% and 18.6% of the soil make up. A table of soil types, acreage of coverage, and percent of the total campus area can be found in Appendix A. The campus sits on an approximately 1200 acre plot and is made up of a central developed and built up area, surrounded by diverse forest communities, agriculture, wetland, and transitional open fields. The northern and eastern parts of the campus forest consist predominantly of maple species (*Acer*) with varying concentration of ash species. Some pine species (*Pinus*) and black locust (*Robinia pseudoacacia*) are also present. The southern part of the campus forest consists of maple, beech (*Fagus*), oak (*Quercus)* and ash. NYSDEC estimates that in Monroe County, and surrounding counties such as Orleans, Genesee, Ontario, Wayne, Seneca, and Livingston,

total basal area is made up of 16% to 28% ash (Figure 2). These counties contain the highest concentration of ash in New York State.

2.2 Imagery

The WorldView-2 satellite is a high-resolution, multispectral sensor, owned by Digital Globe. It provides 1.85m resolution multispectral and 46cm panchromatic resolution imagery at GSD nadir and 770 km altitude. The multispectral sensor collects 8 bands in the follow ranges; 400-450nm, 450-510nm, 510-580nm, 585-625nm, 630-690nm, 705-745nm, 770-895nm, and 860-1040nm (Table 1). WV2 imagery was collected in June (J-WV2) and September (S-WV2) of 2010 of the Rochester Institute of Technology campus. Two datasets, one from each collection date, were used in the study.

Table 1: WorldView-2 wavelength ranges for each of the 8 bands. Near-IR1 and Near-IR2 are near infrared bands.

Coastal:	400-450nm	Red:	630-690nm
Blue:	450-510-nm	Red Edge:	705-745nm
Green:	510-580nm	Near-IR1	770-895nm
Yellow:	585-625nm	Near-IR2	860-1040nm

2.3 Data Collection

Training points were collected between November 2011 and April 2012, when a majority of the forest is in leaf-off. Global Positioning System (GPS) points were collected using a Trimble GeoExplorer 3000 Series GeoXT handheld unit (Trimble Navigation Limited, Sunnyvale, California). The unit was set to record a positional fix every second for ninety seconds and calculate the average position.

Training points were located by walking through the forested areas and selecting representative trees for each class. Sample trees were chosen based on height and crown area, in order to maximize the visible tree cover in satellite imagery. The class of each training point was recorded and a GPS point collected. At each training point, the GPS was held approximately 1 meter above the ground (waist height), and as stationary as possible. During the sampling in April the GPS was mounted to a tripod. During sampling, the GPS was set up on the southern side of the sample tree, and facing the same direction. Training points were categorized into six classes; Ash, Maple, Beech, Oak, Evergreen, and Other. Trees that were used as training points that did not fall into the genus *fraxinus*, *acer*, *quakus*, or *fagus*, and were not *pinales*, were placed into the Other class. The genus was identified using the Peterson Field Guide to Eastern Trees (Petrides and Wehr 1998). In total, 153 training points were recorded consisting of 57 Ash, 52 Maple, 17 Oak, 9 Beech, 11 Evergreen, and 7 Other (Table 2).

Table 2: Number of classification points and test points collected per class.

	CLASSIFICATION	GROUND TRUTH	TOTAL
ASH	40	17	57
MAPLE	37	15	52
OAK	12	5	17
BEECH	6	3	9
EVERGREEN	8	3	11
OTHER	5	2	7
TOTAL	108	45	153

The GPS points were exported into Trimble GPS Pathfinder Office (Trimble Navigation Limited) and differentially corrected. Any points that contained greater than 2.0 meter horizontal error were removed. The points were then exported into ESRI ArcGIS 10.0 as shapefiles.

Within each class, a random selection of approximately 30% of the training points were selected to create a sub-category for use as test points later in the study. The remaining points were used as classification points. Classification points were used in the classification and test points were used for accuracy assessments. A 2.0 meter buffer was created around each point and then exported into ENVI 4.7 (ITT Visual Information Solution, Boulder CO USA) to mimic tree canopies.

2.4 Pre-classification Imagery Preparation

Using ENVI, the J-WV2 and S-WV2 data sets were combined into a single data set using Layer Stacking (LS-WV2). Layer Stacking merges the two data sets by stacking one set of 8 bands on top of another. This provided both temporal and multi-temporal data sets for to test Worldview-2 genus classification abilities.

The classification and training point shapefiles were converted into Region of Interest (ROI) files within ENVI, creating classification ROIs and test ROIs. The forested areas of the campus were manually delineated, using a visual assessment of the imagery. A mask file was created using the delineated areas and was applied to all classifications in order to limit classification confusion with urban areas.

A Principle Component Analysis (PCA) was run on each of the data sets (J-WV2, S-WV2, LS-WV2). The two objectives of using a PCA are to reduce the number of variables and redundancy in the dataset while maintaining variability and to identify hidden patterns and underlying significant variables within the data set. These variables are then classified based upon the amount of information or variability that they explain in the data set. Two PCA data

sets were created from each of the original data sets (J-WV2, S-WV2, LS-WV2). One data set being created used a covariance matrix during the PCA calculation and another used a correlation matrix during the calculation. Table 3 shows the number of variables per data set that were obtained from the PCA.

2.5 Statistical Data Reduction

Spectral signatures were extracted from J-WV2, S-WV2, LS-WV2, and imported into Microsoft Excel. The derivatives were calculated for each of the datasets. The derivative of spectral reflectivity is the rate of change with respect to wavelength (dy/dx) (Rundquist *et al*. 1996). Derivatives were calculated by dividing the difference of successive spectral signatures for each training point by the mean range of the two corresponding bands. The signatures and derivatives were imported into SAS statistical software for analysis. Table 3 shows all of the variables input into SAS. In total 94 variables were evaluated.

A discriminate analysis was first used to identify the spectral signatures that best separate the classes used. This analysis used linear combinations of the variables in order to best explain the data as well as reduce the dimensionality of the data. Significance levels of 0.85, 0.90, 0.95, and 0.99 were evaluated, however little difference was seen in band selection. Therefore 0.85 was used for final analysis. The CORR procedure was used to calculate the correlations between the variables identified by the discriminate analysis. A Pearson correlation coefficient was produced in order to further separate variables if possible. Twelve bands were found and selected for grouping into a new data set called RD-WV2. The bands that were selected can be found in Table 3a-c, as well as the remaining other bands used in the statistical analysis.

Table 3: This table shows the number of variables that were used in the discriminant analysis for each of the data sets. For the June and September data set unaltered (Raw) imagery and the spectral derivatives (Deriv) were used. A Principle Component Analysis using a covariance matrix (PCA – Cov) and a correlation matrix (PCA – Cor) were included. Shaded cells show the variables selected for the RD-WV2 data set.

a.

June Worldview-2 Data set

Raw	Derivative	PCA - Cov	PCA - Cor
JUN_BAND_1	JUN_Deriv_1	PCAJ_2_BAND_1	PCAJ_4_BAND_1
JUN_BAND_2	JUN_Deriv_2	PCAJ_2_BAND_2	PCAJ_4_BAND_2
JUN_BAND_3	JUN_Deriv_3	PCAJ_2_BAND_3	PCAJ_4_BAND_3
JUN_BAND_4	JUN_Deriv_4	PCAJ_2_BAND_4	PCAJ_4_BAND_4
JUN_BAND_5	JUN_Deriv_5	PCAJ_2_BAND_5	PCAJ_4_BAND_5
JUN_BAND_6	JUN_Deriv_6	PCAJ_2_BAND_6	PCAJ_4_BAND_6
JUN_BAND_7	JUN_Deriv_7	PCAJ_2_BAND_7	PCAJ_4_BAND_7
JUN_BAND_8		PCAJ_2_BAND_8	PCAJ_4_BAND_8

b.

September Worldview-2 Data set

Raw	Derivative	PCA - Cov	PCA - Cor
SEP_BAND_1	SEP_Deriv_1	PCAS_2_BAND_1	PCAS_4_BAND_1
SEP_BAND_2	SEP_Deriv_2	PCAS_2_BAND_2	PCAS_4_BAND_2
SEP_BAND_3	SEP_Deriv_3	PCAS_2_BAND_3	PCAS_4_BAND_3
SEP_BAND_4	SEP_Deriv_4	PCAS_2_BAND_4	PCAS_4_BAND_4
SEP_BAND_5	SEP_Deriv_5	PCAS_2_BAND_5	PCAS_4_BAND_5
SEP_BAND_6	SEP_Deriv_6	PCAS_2_BAND_6	PCAS_4_BAND_6
SEP_BAND_7	SEP_Deriv_7	PCAS_2_BAND_7	PCAS_4_BAND_7
SEP_BAND_8		PCAS_2_BAND_8	PCAS_4_BAND_8

c.

June-September Layer Stacked Data set

PCA - Cov	PCA - Cor
PCALS_2_BAND_1	PCALS_4_BAND_1
PCALS_2_BAND_2	PCALS_4_BAND_2
PCALS_2_BAND_3	PCALS_4_BAND_3
PCALS_2_BAND_4	PCALS_4_BAND_4
PCALS_2_BAND_5	PCALS_4_BAND_5
PCALS_2_BAND_6	PCALS_4_BAND_6
PCALS_2_BAND_7	PCALS_4_BAND_7
PCALS_2_BAND_8	PCALS_4_BAND_8
PCALS_2_BAND_9	PCALS_4_BAND_9
PCALS_2_BAND_10	PCALS_4_BAND_10
PCALS_2_BAND_11	PCALS_4_BAND_11
PCALS_2_BAND_12	PCALS_4_BAND_12
PCALS_2_BAND_13	PCALS_4_BAND_13
PCALS_2_BAND_14	PCALS_4_BAND_14
PCALS_2_BAND_15	PCALS_4_BAND_15
PCALS_2_BAND_16	PCALS_4_BAND_16

2.6 Spectral Analysis

2.6.1 Classification Types

A maximum likelihood analysis was chosen for the classification method. In a maximum likelihood classification (MLC), pixels are classified using a probability function and training site inputs, and designate a class based upon the probability of belong to that class (Erener 2013).A detailed explanation of the methodology and principles behind the MLC can be found in Myung 2003.

Three different classification groups were tested, consisting of class groupings of six class (6C), two classes (2C) and five classes (5C). 6C comprised the classes Ash, Maple, Oak, Beech, Evergreen, and Other. 2C involved the merger of the Maple, Oak, Beech, Evergreen and Other classes in a single class and Ash remaining as its own class. As a result of some confusion between the Ash and Maple classes during some preliminary research, we merged the Ash and Maple classes into a single class, leaving the four remaining classes (Oak, Beech, Evergreen, Other).

Formatted: Condensed by 0.2 pt

2.6.2 Classification Procedure

The MLC was run on the J-WV2, S-WV2, LS-WV2, and RD-WV2 datasets. A probability threshold of 0.85 was selected, so any pixel that had lower than an 85% probability of being classified as one of the classes remained unclassified. Each classification (6C, 2C, 5C) was run on each of the data sets. The accuracy of each classification was calculated by using the test ROIs and confusion matrix. Each confusion matrix output consisted of an overall accuracy assessment and kappa coefficient, individual class accuracies, errors of commission and omission, and producer and user accuracies (Appendix A).

3. Results

Table 4 displays the results of the three different classifications (2C, 5C, 6C) performance using the four data sets analyzed (J-WV2, S-WV2, LS-WV2, RD-WV2) for the ash and maple class. The 6C classification yielded the highest accuracy for classifying both ash and maple when run using the RD-WV2 data set. Ash test pixels were classified correctly 72.22% of the time and maple test pixels 52.94%. This same combination also yielded the lowest ash being misclassified as maple (22.22%) and maple being misclassified as ash (23.53%).

Table 4: This table displays the percent accuracy of the ash, maple and combined ash-maple classes for Worldview-2 imagery collected in June and September 2010 (J-WV2 and S-WV2), a layer stacked data set of J-WV2 and S-WV2 (LS-WV2), and a statistically reduced data set (RD-WV2). The percent that ash was miss-classified as maple of vice versa is in brackets.

Class	**J-WV2**	**S-WV2**	**LS-WV2**	**RD-WV2**
Ash (6C)	53.70 (24.07)	50.00 (27.78)	61.11 (33.33)	72.22 (22.22)
Maple (6C)	41.18 (27.45)	31.37 (23.53)	47.06 (41.18)	52.94 (23.53)
Ash-Maple (5C)	64.76	63.81	89.52	80.95
Ash (2C)	70.37	55.56	61.11	81.48

The S-WV2 data set yielded the lowest accuracy for ash and maple at a percent of 50.00% and 31.37% respectively. Ash only saw a small increase of less than 4.00% accuracy for the J-WV2 data set, 53.70%, while the maple class accuracy increased by approximately 10.00% to 41.18% (Table 4). There were not significant differences between J-WV2 and S-WV2 in terms of ash and maple being incorrectly classified as the other.

The apparent confusion occurring between the ash and maple classes prompted further investigation. The ash and maple classes were merged to determine if the confusion was between

classes another unknown variable. The 5C classification resulted in significantly higher accuracies overall for all data sets investigated. LS-WV2 yielded the highest accuracy of 89.52%. RD-WV2 resulted in a slightly lower accuracy of 80.95%, however still a higher accuracy then when using the 6C classification. J-WV2 and S-WV2 performed similarly with accuracies of 64.76% and 63.81% respectively (Table 4).

To further determine if the classification confusion was a result of a spectral similarity between the ash and maple classes; the maple, beech, oak, and other classes were merged together. The 2C classification yielded a high accuracy of 81.48% when using the RD-WV2 dataset. J-WV2 resulted in the next highest accuracy with 70.37%. The LS-WV2 and S-WV2 datasets produced accuracies of 61.11% and 55.56% respectively (Table 4). The overall, class, producer, and user accuracies for all the variables can be found in Appendix B, Tables 1-8.

4. Discussion

4.1 Classification analysis

Classification accuracies varied depending upon the dataset and classification used. Within the 6C classification there was a pattern of consistent identification confusion between the ash and maple classes (Table 4). While it is expected to have some amount of classification error, 20-35% of the ash test pixels were misclassified as maple, depending upon the data set. Misclassification of ash as any of the other classes, for example oak, was not significant compared to the proportion confused with maple. This confusion is also seen in the maple classification, where there is a consistent misclassification of maple as ash for a large proportion of the test pixels.

The 2C classification was used to determine if the confusion that was occurring was from the maple class itself or from some other factor. Class accuracy for ash did increase compared to the 6C classification, depending upon the data set (Table 4). The RD-WV2 and S-WV2 data sets showed small increases in accuracy while the J-WV2 data set greatly improved. However the LS-WV2 data set showed no change.

When the ash and maple classes were merged, this new class resulted in a significantly higher accuracy when using the LS-WV2 data set (Table 4). This was the highest accuracy that was found throughout the study for the ash or maple classes.

Ash was best identified using the RD-WV2 dataset and the 2C classification, at an accuracy of 81.48% (Table 4). While the 5C classification produced a higher accuracy of 89.52%, any pixel designated within the Ash-Maple class could be either genus, making specific

identification impossible. While the classification of ash using the 6C classification resulted in a lower accuracy of 72.22% with the RD-WV2 dataset, making it slightly too low for commercial purposes, other classes such as evergreen and oak were identified to an accuracy of 100.00% using the same dataset.

The reasons for this confusion between the ash and maple classifiers can be attributed to a number of possibilities. Worldview-2 multispectral pixel size is 1.85x1.85m (Appendix A). While smaller than other multispectral sensors such as Landsat TM and BGIS 2000, it is possible that the mixed nature of the forest community and varying canopy sizes are causing pixels on the edge of tree canopies to confuse the classification. Also, the varying canopy heights and tree spacing might be causing shadows and ground spectral signatures to confuse the classification. Additionally, the spectral signatures of ash and maple are fairly similar in both the June and September datasets (Figure 12). From an ecological stand point, it is not uncommon to find ash and maple occupying the same forest cover areas such as Sugar Maple stands and Black Ash, American Elm, Red Maple stands (USFS). Also, structurally, both species have opposite branching patterns, which may lead to similar spectral signatures.

4.2 Multi-temporal Analysis

Overall and individual class accuracy differences between single date and multi-temporal (LS-WV2) data sets showed some pattern. In general, the overall accuracy of the J-WV2 and S-WV2 datasets were lower than of the LS-WV2 data set. The S-WV2 dataset overall accuracy was higher than that of the LS-WV2 data set using the 2C classification, 72,73% and 71.43% respectively. Within the ash class specifically, multi-temporal data resulted in higher accuracy using the 6C and 5C classifications. However, using the 2C classification, the J-WV2 data set

produced the higher accuracy, 70.37% compared to 61.11% for the LS-WV2 data set.

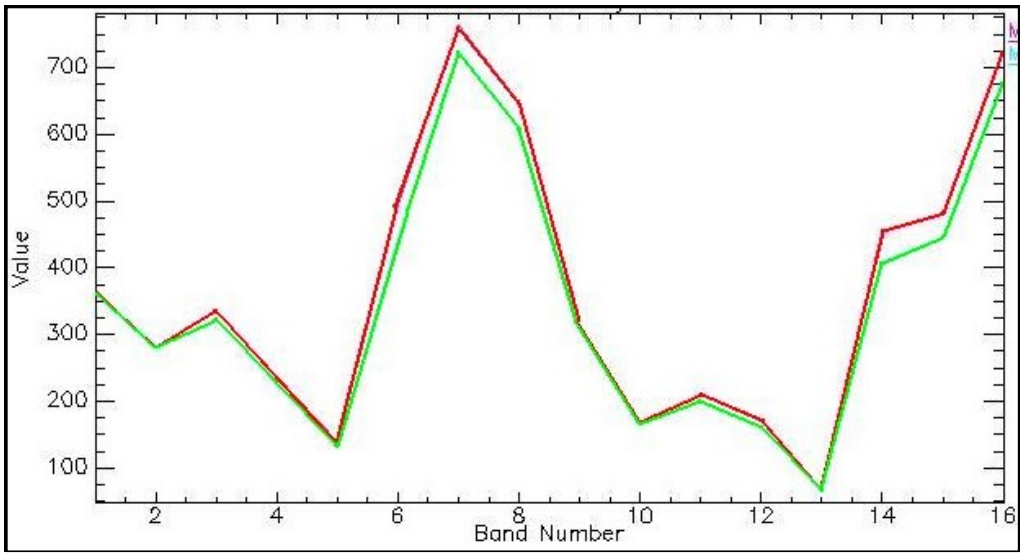

Figure 12: Shows the spectral signature for ash (green) and maple (red) for the layer stacked dataset. Bands 1 through 8 are from the June WorldView-2 dataset and bands 9 through 16 are from the September WorldView-2 dataset.

Multi-temporal imagery improved classification accuracy of ash and maple for almost all classifications. The one exception was the J-WV2 data set combined with the 2C classification that had an accuracy of 70.37%, compared to the L-WV2 data set accuracy of 61.11%. These results show that multi-temporal imagery has a positive impact on classification accuracy, depending upon the classification that is used and the specific class that is in question. The literature shows that this has also been the case with other classification studies (Key *et al*.2001, Ghioca-Robrecht *et al*. 2008, Townsend and Walsh 2001, Hill *et al*. 2010).

The improved accuracy results from the multi-temporal analysis point to possible further accuracy enhancements with additional imagery from other times of the growing season. Research has shown that multi-temporal imagery can improve classification accuracy (Wolter *et*

al. 1995, Key *et al*. 2001, Singh and Glen 2009, Townsend and Walsh 2001). Additionally, the use of different types of multispectral imagery, for example a combination of Landsat TM and SPOT HRG, should be investigated (Lu *et al*. 2008, Miguel-Ayanz and Biging 1997).

Given the mixed nature of the forest, high resolution imagery might be able to better differentiate individual tree genus due to less confusion with surroundings. Hyperspectral imagery offers a promising possibility with its narrow band ranges and high resolution (Jones *et al*. 2010, Yang and Everitt 2010, Lui *et al*. 2012). The inclusion of LiDAR data to delineate canopy and structure combined with multispectral imagery has produced favorable classification results (Ke *et al*. 2010, Cho *et al*. 2012, Dinuls *et al*. 2012).

4.3 Ecological Impacts

The type of impacts that the EAB infestation will have on the forest community both on the RIT campus and in the region in general is not clear. The EAB has been in the United States since at least 2005, particularly in Michigan, where the invasion is believed to have originated (Kovacs *et al*. 2010). Now that stands of ash have been decimated and forest regeneration has begun, initial inferences can be drawn on forest community impacts. Kashian and Witter (2011) investigated the potential for ash re-establishment in Lower Michigan. The authors found that while overstory ash mortality was almost 100%, there were abundant understory ash populations. However, there were indications that the seed bank was becoming depleted, as seedlings 1-2 years were the least abundant. They also suggested that overstory competition with other species was a key driver of ash regeneration, and that the influence that the EAB may have is unknown at this time. While the species composition in the previous study was different from that of this study, it could be assumed that similar effects may be seen.

Due to the limited amount of research that has been conducted on the role that ash play in a forest ecosystem, it is difficult to state with any certainty what impact the loss of ash may have on the forest community. However, some inferences can be made based upon a few studies. A study by Petritan *et al* (2009) investigated the growth response of ash, maple, and beech sapling to disturbance opening in the canopy. Ash and maple were characterized as "gap species", due to rapid growth as a result of increased light availability following an opening in the canopy. Beech displayed more shade tolerant characteristics and did not compete as well for new canopy space. Based upon this study it would appear when a gap opens up in the canopy, such as the death of a mature overstory tree, ash and maple would compete. This competition with the presence of the EAB could inhibit ash reaching a mature stage and leading to an increase in maple populations.

Parallels can be drawn between the possible regeneration response of ash to the EAB infestation and the response seen in chestnut mortality as a result of the chestnut blight. The chestnut has been reduced to an understory shrub due to the chestnut blight killing trees before they can reach full maturity (Ellison *et al*. 2005). EAB commonly infest tree of 5-9cm in DBH and rarely smaller trees (Wang *et al*. 2010). Much like the chestnut blight, greater age or size increases the likelihood of infestation. So ash may be relegated to an understory role.

The impact that large scale ash mortality may have on the forest community is also unclear. Ulyshen *et al* (2011) assessed the impact that the increase in canopy gaps and fallen ash trees has on the arthropods and exotic earthworms in a forest experiencing EAB infestation. The authors found that litter dwelling taxa were more abundant near fallen logs, regardless of canopy openness. Therefore, the initial die off of RIT ash would probably have a positive effect on the detritivores on campus, but it remains to be seen what the long term affects might be.

5. Conclusions

This study looked to determine the feasibility of Worldview-2 data for classifying a mixed deciduous forest at a genus level with the focus on ash populations for EAB monitoring and management purposes. This methodology and the data sets produced good classification accuracy for ash, 81.48% (Table 4). The results seen in this study are consistent with some of the literature regarding the use of Worldview-2 imagery for forest classification purposes (Abd et al. 2012; Immitzer et al., 2012). Higher accuracy was achieved when the ash and maple classes were merged, yielding a class accuracy of 89.53% (Table 4). Analysis of the results indicate that confusion between classifiers, particularly ash and maple, were a key reason for lower classification accuracy. The very mixed nature of the forest community, where pure stands are uncommon, combined with the resolution of Worldview-2 imagery (1.85x1.85m) may have cause pixel mixing and confusion.

While the classification of ash was not to an accuracy level that would be ideal for monitoring purposes, it was accurate enough to assist in guiding field surveys and investigations. This study was conducted on a small scale and could likely be scaled up to potentially classify areas of ash that could be inspected for possible EAB infestation. This study was conducted in a relatively small area, where access for field surveys was available. In areas where ash populations are less accessible, remote sensing can play an important role in locating and prioritizing monitoring efforts. Parks would be a particular target of interest for monitoring, given that infested firewood transportation is one of the key modes of EAB spread, and firewood use in parks is obvious. Knowing the areas and extent of ash populations in large forested areas, such as parks, is important for monitoring and management of EAB.

Remote sensing has the potential to offer more than simply locating and identify populations of ash. There is a considerable body of research involving the use of remote sensing for evaluating plant stress (Holer, Dockray, Barber, 1983; Sepculcre-Canto et al., 2006; Asmaryan et al., 2013). Part of the difficulty in monitoring EAB infestation and spread is that symptoms of infestation are not readily apparent until too late. Subtle spectral changes in leaf reflectance can indicate plant stress due to a variety of factors such as water or soil. Most importantly, plant stress can be a result of infestation. Locating ash populations and then assessing the corresponding stress levels via remote sensing could greatly focus field investigations.

Formatted: Condensed by 0.2 pt

Other multispectral imaging apparatus such as Landsat TM, Quickbird, and IKONOS offer additional data source for use in combination with Worldview-2. The improvement seen in classification accuracy with multi-temporal data would indicate that increasing the number of collection dates utilized may further improve the model. Hyperspectral imagery and LiDAR data, in combination with Worldview-2 or separately, offer additional classification capabilities. The unique spectral signature of ash could be extracted from hyperspectral imageries enormous volume of narrow spectral range bands. LiDAR could potentially identify structural characteristics of ash, improving accuracy capabilities.

The importance of ash in its respective habitats is unclear, as is the impact that the emerald ash borer may have in the long term as cleared ash stands begin to regenerate. These unknowns hinder attempts at projecting the influence that the emerald ash borer will have on the ash population and ecosystem. With gaps opening up in forest canopies as ash trees die, competition from other forest tree species, such as maple, could inhibit population regeneration.

Ash is just beginning to regenerate in Michigan from the initial EAB infestations. How the ash population responds to this invasion will be important for predicting local ash population impacts.

Formatted: Condensed by 0.1 pt

More research is necessary in order to further understand the reason for the confusion between ash and maple, the potential for alternative forms of remote sensing for ash classification, and the ecological and economic impacts of the EAB infestation. Remote sensing can play a key role in both managing and preventing present and future invasions.

Appendix A

Monroe County, New York (NY055)			
Map Unit Symbol	Map Unit Name	Acres in AOI	Percent of AOI
ArB	Arkport very fine sandy loam, 0 to 6 percent slopes	4.1	0.3%
Ca	Canandaigua silt loam	282.1	23.4%
CeA	Cayuga silt loam, 0 to 2 percent slopes	4.0	0.3%
CeB	Cayuga silt loam, 2 to 6 percent slopes	69.2	5.7%
ChA	Churchville silt loam, 0 to 2 percent slopes	9.7	0.8%
ChB	Churchville silt loam, 2 to 6 percent slopes	2.5	0.2%
CkA	Claverack loamy fine sand, 0 to 2 percent slopes	28.2	2.3%
CkB	Claverack loamy fine sand, 2 to 6 percent slopes	78.2	6.5%
ClA	Collamer silt loam, 0 to 2 percent slopes	4.0	0.3%
ClB	Collamer silt loam, 2 to 6 percent slopes	6.2	0.5%
CoB	Colonie loamy fine sand, 0 to 6 percent slopes	36.3	3.0%
CoC	Colonie loamy fine sand, 6 to 12 percent slopes	1.1	0.1%
Cu	Cosad loamy fine sand	52.1	4.3%
Ee	Eel silt loam	10.5	0.9%
ElA	Elnora loamy fine sand, 0 to 2 percent slopes	50.6	4.2%
GaA	Galen very fine sandy loam, 0 to 2 percent slopes	7.8	0.6%
GaB	Galen very fine sandy loam, 2 to 6 percent slopes	9.2	0.8%
HfA	Hilton fine sandy loam, 0 to 3 percent slopes	2.9	0.2%
HlA	Hilton loam, 0 to 3 percent slopes	2.2	0.2%
Le	Lakemont silt loam	33.8	2.8%
Ng	Niagara silt loam	223.9	18.6%
OdA	Odessa silt loam, 0 to 2 percent slopes	104.4	8.7%
OdB	Odessa silt loam, 2 to 6 percent slopes	19.7	1.6%
OfB	Ontario fine sandy loam, 3 to 8 percent slopes	67.4	5.6%
OfC	Ontario fine sandy loam, 8 to 15 percent slopes	8.9	0.7%
OnB	Ontario loam, 3 to 8 percent slopes	27.9	2.3%
OnC	Ontario loam, 8 to 15 percent slopes	19.1	1.6%
OnF	Ontario loam, 25 to 60 percent slopes	0.1	0.0%
RgB	Riga silt loam, 2 to 8 percent slopes	4.9	0.4%
SeA	Schoharie silt loam, 0 to 2 percent slopes	5.3	0.4%
SeB	Schoharie silt loam, 2 to 6 percent slopes	15.2	1.3%
W	Water	4.7	0.4%
Wg	Wayland silt loam	10.8	0.9%
Totals for Area of Interest		**1,206.8**	**100.0%**

Figure 1: Soil type and proportion of the Rochester Institute of Technology area, derived from the USGS Websoil Survey.

BGIS 2000 Mission Suitability

Item	*BGIS 2000 Performance*
Spatial Resolution	Panchromatic: ~0.5 to 1.25 m ground sample distance (GSD) or 1.37 mrad Multispectral: ~2 to 5 m GSD or 5.47 mrad for 4 VNIR bands (Landsat-like)
Ground Swath Width	2.12 degrees cross track (14 to 34 km depending on altitude
Geolocation	<15 m (3-sigma) after ground processing
Data Acquisition Modes	Pushbroom imaging system is capable of obtaining: Square images Elongated strip images Mosaic patterns Stereo pairs within single pass
Operations	Simultaneous imaging and data transmission capability
Onboard Storage Capacity	Scalable up to 200 Gbits (equivalent to over 90 square images)
Data Compression bit initial quantization	Average 2 bits per pixel from 11
Calibration	<10 % absolute
Pointing Accuracy	<0.5 milliradians absolute per axis (200 to 450 m)
Agility (along and cross track)	Time to re-point and stabilize the spacecraft for imaging: Maneuver of 10 degrees in 20 seconds Maneuver of 50 degrees in 45 seconds
Communications Image Data Housekeeping	 320 Mbps X-band S- or X-band from 4 to 256 Kbps 2 Kbps S-band uplink
Design Life	>5 years achieved with redundant architecture
Orbit Options	400 to 900 km 0 degrees to sun synchronous
Launch Vehicles	COSMOS SL-8, Taurus, Athena, Titan II, Long March
Spacecraft Mass	931 kg (wet)
Propulsion	Anhydrous Hydrazine (N_2H_4) blowdown

Note: Numerical ranges reflect orbit altitude options (400 km to 900 km)

Figure 2: Woldview-2 satellite specifications (Digital Globe).

Appendix B

Table 1: Shows the overall accuracy and kappa values for each type of classification and dataset combination analyzed.

Data Set	OA (%)	Kappa
June (6C)	48.05	0.3207
September (6C)	43.51	0.2775
Layer Stack (6C)	50.00	0.3049
Reduced Data (6C)	70.13	0.6100
June (5C)	67.53	0.4863
September (5C)	66.23	0.4829
Layer Stack (5C)	73.38	0.4257
Reduced Data (5C)	72.73	0.5070
June (2C)	67.53	0.3378
September (2C)	72.73	0.4079
Layer Stack (2C)	71.43	0.3779
Reduced Data (2C)	79.22	0.5659

Table 2: These four tables display the individual class accuracy for each of the datasets used with the 6C classification. a, b, c, and d correspond to the J-WV2, S-WV2, LS-WV2 , and RD-WV2 datasets respectively.

a.

Class	Evergreen	Ash	Beech	Maple	Oak	Other	Total
Unclassified	0.00	0.00	0.00	0.00	0.00	0.00	0.00
Evergreen	77.78	1.85	0.00	0.00	0.00	0.00	5.19
Ash	11.11	53.70	0.00	27.45	0.00	35.71	31.82
Beech	0.00	0.00	40.00	7.84	6.25	0.00	5.84
Maple	0.00	24.07	30.00	41.18	0.00	21.43	25.97
Oak	0.00	18.52	10.00	7.84	68.75	28.57	19.48
Other	11.11	1.85	20.00	15.69	25.00	14.29	11.69
Total	100.00	100.00	100.00	100.00	100.00	100.00	100.00

b.

Class	Evergreen	Ash	Beech	Maple	Oak	Other	Total
Unclassified	0.00	0.00	0.00	0.00	0.00	0.00	0.00
Evergreen	55.56	7.41	0.00	9.80	6.25	0.00	9.74
Ash	11.11	50.00	10.00	23.53	0.00	0.00	26.62
Beech	0.00	0.00	20.00	3.92	12.50	21.43	5.84
Maple	33.33	27.78	20.00	31.37	12.50	14.29	25.97
Oak	0.00	3.70	50.00	19.61	62.50	14.29	18.83
Other	0.00	11.11	0.00	11.76	6.25	50.00	12.99
Total	100.00	100.00	100.00	100.00	100.00	100.00	100.00

c.

Class	Evergreen	Ash	Beech	Maple	Oak	Other	Total
Unclassified	0.00	0.00	0.00	0.00	0.00	0.00	0.00
Evergreen	55.56	1.85	0.00	0.00	0.00	0.00	3.90
Ash	0.00	61.11	10.00	41.18	6.25	7.14	37.01
Beech	0.00	0.00	0.00	0.00	0.00	0.00	0.00
Maple	44.44	33.33	60.00	47.06	12.50	42.86	38.96
Oak	0.00	1.85	30.00	1.96	56.25	7.14	9.74
Other	0.00	1.85	0.00	9.80	25.00	42.86	10.39
Total	100.00	100.00	100.00	100.00	100.00	100.00	100.00

d.

Class	Evergreen	Ash	Beech	Maple	Oak	Other	Total
Unclassified	0.00	0.00	0.00	0.00	0.00	0.00	0.00
Evergreen	100.00	1.85	0.00	1.96	0.00	0.00	7.14
Ash	0.00	72.22	0.00	23.53	0.00	0.00	33.12
Beech	0.00	0.00	90.00	5.88	0.00	7.14	8.44
Maple	0.00	22.22	0.00	52.94	0.00	0.00	25.32
Oak	0.00	1.85	10.00	7.84	100.00	35.71	17.53
Other	0.00	1.85	0.00	7.84	0.00	57.14	8.44
Total	100.00	100.00	100.00	100.00	100.00	100.00	100.00

Table 3: These four tables display the individual class accuracy for each of the datasets used with the 5C classification. a, b, c, and d correspond to the J-WV2, S-WV2, LS-WV2 , and RD-WV2 datasets respectively.

a.

Class	Evergreen	Ash-Maple	Beech	Oak	Other	Total
Unclassified	0.00	0.00	0.00	0.00	0.00	0.00
Evergreen	88.89	2.86	0.00	0.00	0.00	7.14
Ash-Maple	0.00	64.76	0.00	0.00	35.71	47.40
Beech	0.00	7.62	90.00	6.25	14.29	12.99
Oak	0.00	14.29	10.00	87.50	14.29	20.78
Other	11.11	10.48	0.00	6.25	35.71	11.69
Total	100.00	100.00	100.00	100.00	100.00	100.00

b.

Class	Evergreen	Ash-Maple	Beech	Oak	Other	Total
Unclassified	0.00	0.95	0.00	0.00	0.00	0.65
Evergreen	88.89	8.57	0.00	0.00	0.00	11.04
Ash-Maple	11.11	63.81	0.00	0.00	0.00	44.16
Beech	0.00	4.76	70.00	25.00	21.43	12.34
Oak	0.00	11.43	30.00	75.00	21.43	19.48
Other	0.00	10.48	0.00	0.00	57.14	12.34
Total	100.00	100.00	100.00	100.00	100.00	100.00

c.

Class	Evergreen	Ash-Maple	Beech	Oak	Other	Total
Unclassified	0.00	0.00	0.00	0.00	0.00	0.00
Evergreen	55.56	0.00	0.00	0.00	0.00	3.25
Ash-Maple	44.44	89.52	70.00	18.75	57.14	75.32
Beech	0.00	0.00	0.00	0.00	0.00	0.00
Oak	0.00	3.81	30.00	56.25	7.14	11.04
Other	0.00	6.67	0.00	25.00	35.71	10.39
Total	100.00	100.00	100.00	100.00	100.00	100.00

d.

Class	Evergreen	Ash-Maple	Beech	Oak	Other	Total
Unclassified	0.00	0.00	0.00	0.00	0.00	0.00
Evergreen	66.67	1.90	0.00	0.00	0.00	5.19
Ash-Maple	33.33	80.95	20.00	12.50	7.14	60.39
Beech	0.00	2.86	30.00	12.50	7.14	5.84
Oak	0.00	5.71	40.00	68.75	35.71	16.88
Other	0.00	8.57	10.00	6.25	50.00	11.69
Total	100.00	100.00	100.00	100.00	100.00	100.00

Table 4: These four tables display the individual class accuracy for each of the datasets used with the 2C classification. a, b, c, and d correspond to the J-WV2, S-WV2, LS-WV2 , and RD-WV2 datasets respectively.

a.

Class	Ash	Others	Total
Unclassified	0.00	0.00	0.00
Ash	70.37	34.00	46.75
Others	29.63	66.00	53.25
Total	100.00	100.00	100.00

b.

Class	Ash	Others	Total
Unclassified	7.41	0.00	2.60
Ash	55.56	18.00	31.17
Others	37.04	82.00	66.23
Total	100.00	100.00	100.00

c.

Class	Ash	Others	Total
Unclassified	0.00	0.00	0.00
Ash	61.11	23.00	36.36
Others	38.89	77.00	63.64
Total	100.00	100.00	100.00

d.

Class	Ash	Others	Total
Unclassified	0.00	0.00	0.00
Ash	81.48	22.00	42.86
Others	18.52	78.00	57.14
Total	100.00	100.00	100.00

Table 6: These four tables display the commission, omission, producer accuracy, and user accuracy for each of the datasets used with the 6C classification. a, b, c, and d correspond to the J-WV2, S-WV2, LS-WV2 , and RD-WV2 datasets respectively.

a.

Class	Commission	Omission	Prod. Acc.	User Acc.
Evergreen	12.50	22.22	77.78	87.50
Ash	40.82	46.30	53.70	59.18
Beech	55.56	60.00	40.00	44.44
Maple	47.50	58.82	41.18	52.50
Oak	63.33	31.25	68.75	36.67
Other	88.89	85.71	14.29	11.11

b.

Class	Commission	Omission	Prod. Acc.	User Acc.
Evergreen	66.67	44.44	55.56	33.33
Ash	34.15	50.00	50.00	65.85
Beech	77.78	80.00	20.00	22.22
Maple	60.00	68.63	31.37	40.00
Oak	65.52	37.50	62.50	34.48
Other	65.00	50.00	50.00	35.00

c.

Class	Commission	Omission	Prod. Acc.	User Acc.
Evergreen	16.67	44.44	55.56	83.33
Ash	42.11	38.89	61.11	57.89
Beech	0.00	100.00	0.00	0.00
Maple	60.00	52.94	47.06	40.00
Oak	40.00	43.75	56.25	60.00
Other	62.50	57.14	42.86	37.50

d.

Class	Commission	Omission	Prod. Acc.	User Acc.
Evergreen	18.18	0.00	100.00	81.82
Ash	23.53	27.78	72.22	76.47
Beech	30.77	10.00	90.00	69.23
Maple	30.77	47.06	52.94	69.23
Oak	40.74	0.00	100.00	59.26
Other	38.46	42.86	57.14	61.54

Table 7: These four tables display the commission, omission, producer accuracy, and user accuracy for each of the datasets used with the 5C classification. a, b, c, and d correspond to the J-WV2, S-WV2, LS-WV2 , and RD-WV2 datasets respectively.

a.

Class	Commission	Omission	Prod. Acc.	User Acc.
Evergreen	20.27	11.11	88.89	72.73
AshMaple	6.85	35.24	64.76	93.15
Beech	55.00	10.00	90.00	45.00
Oak	56.25	12.50	87.50	43.75
Other	72.22	64.29	35.71	27.78

b.

Class	Commission	Omission	Prod. Acc.	User Acc.
Evergreen	72.73	25.00	75.00	27.27
AshMaple	6.00	44.71	55.29	94.00
Beech	100.00	100.00	0.00	0.00
Oak	64.00	25.00	75.00	36.00
Other	85.00	40.00	60.00	15.00

c.

Class	Commission	Omission	Prod. Acc.	User Acc.
Evergreen	0.00	44.44	55.56	100.00
AshMaple	18.97	10.48	89.52	81.03
Beech	0.00	100.00	0.00	0.00
Oak	47.06	43.75	56.25	52.94
Other	68.75	64.29	35.71	31.25

d.

Class	Commission	Omission	Prod. Acc.	User Acc.
Evergreen	25.00	33.33	66.67	75.00
Ash-Maple	8.60	19.05	80.95	91.40
Beech	66.67	70.00	30.00	33.33
Oak	57.69	31.25	68.75	42.31
Other	61.11	50.00	50.00	38.89

Table 8: These four tables display the commission, omission, producer accuracy, and user accuracy for each of the datasets used with the 2C classification. a, b, c, and d correspond to the J-WV2, S-WV2, LS-WV2 , and RD-WV2 datasets respectively.

a.

Class	Commission	Omission	Prod. Acc.	User Acc.
Ash	47.22	29.63	70.37	52.78
Others	19.51	34.00	66.00	80.49

b.

Class	Commission	Omission	Prod. Acc.	User Acc.
Ash	37.50	44.44	55.56	62.50
Others	19.61	18.00	82.00	80.39

c.

Class	Commission	Omission	Prod. Acc.	User Acc.
Ash	41.07	38.89	61.11	58.93
Others	21.43	23.00	77.00	78.57

d.

Class	Commission	Omission	Prod. Acc.	User Acc.
Ash	33.33	18.52	81.48	66.67
Others	11.36	22.00	78.00	88.64

Bibliography

Anulewicz, A. C., D. G. McCullough, D. L. Cappaert, and T. M. Poland. "Host Range of the Emerald Ash Borer (Agrilus Planipennis Fairmaire) (Coleoptera : Buprestidae) in North America: Results of Multiple-Choice Field Experiments." [In English]. *Environmental Entomology* 37, no. 1 (Feb 2008): 230-41.

Asmaryan, S., T. A. Warner, V. Muradyan, and G. Nersisyan. "Mapping Tree Stress Associated with Urban Pollution Using the Worldview-2 Red Edge Band." *Remote Sensing Letters* 4, no. 2 (2013): 200-09.

BenDor, Todd K. Todd K. "Modeling the Spread of the Emerald Ash Borer." *Ecological modelling* 197, no. 1/2 (2006).

Berni, Jose A. J., Pablo J. Zarco-Tejada, Lola Suarez, and Elias Fereres. "Thermal and Narrowband Multispectral Remote Sensing for Vegetation Monitoring from an Unmanned Aerial Vehicle." *Ieee Transactions on Geoscience and Remote Sensing* 47, no. 3 (Mar 2009): 722-38.

Campbell, James B., and Randolph H. Wynne. *Introduction to Remote Sensing*. The Guilford Press, 2011.

Davis, Mark A., Mathew K. Chew, Richard J. Hobbs, Ariel E. Lugo, John J. Ewel, Geeret J. Vermeij, James H. Brown*, et al.* "Don't Judge Species on Their Origins." *Nature* 474 (2011): 153-54.

Dinuls, R., G. Erins, A. Lorencs, I. Mednieks, and J. Sinica-Sinavskis. "Tree Species Identification in Mixed Baltic Forest Using Lidar and Multispectral Data." [In English]. *Ieee Journal of Selected Topics in Applied Earth Observations and Remote Sensing* 5, no. 2 (Apr 2012): 594-603.

Duan, J. J., R. W. Fuester, J. Wildonger, P. B. Taylor, S. Barth, and S. E. Spichiger. "Parasitoids Attacking the Emerald Ash Borer (Coleoptera: Buprestidae) in Western Pennsylvania." [In English]. *Florida Entomologist* 92, no. 4 (Dec 2009): 588-92.

Duan, J. J., P. B. Taylor, and R. W. Fuester. "Biology and Life History of Balcha Indica, an Ectoparasitoid Attacking the Emerald Ash Borer, Agrilus Planipennis, in North America." [In English]. *Journal of Insect Science* 11 (Sep 2011): 9.

Ellison, A. M., M. S. Bank, B. D. Clinton, E. A. Colburn, K. Elliott, C. R. Ford, D. R. Foster*, et al.* "Loss of Foundation Species: Consequences for the Structure and Dynamics of Forested Ecosystems." [In English]. *Frontiers in Ecology and the Environment* 3, no. 9 (Nov 2005): 479-86.

Erener, A. "Classification Method, Spectral Diversity, Band Combination and Accuracy Assessment Evaluation for Urban Feature Detection." [In English]. *International Journal of Applied Earth Observation and Geoinformation* 21 (Apr 2013): 397-408.

Ghioca-Robrecht, D. M., C. A. Johnston, and M. G. Tulbure. "Assessing the Use of Multiseason Quickbird Imagery for Mapping Invasive Species in a Lake Erie Coastal Marsh." [In English]. *Wetlands* 28, no. 4 (Dec 2008): 1028-39.

Griffith, Randy Scott. "Fraxinus Americana. In: Fire Effects Information System." http://www.fs.fed.us/database/feis/: U.S. Department of Agriculture, Forest Service, 1991.

Horler, D. N. H., M. Dockray, and J. Barber. "The Red Edge of Plant Leaf Reflectance." [In English]. *International Journal of Remote Sensing* 4, no. 2 (1983): 273-88.

Jones, Trevor G., Nicholas C. Coops, and Tara Sharma. "Assessing the Utility of Airborne Hyperspectral and Lidar Data for Species Distribution Mapping in the Coastal Pacific Northwest, Canada." *Remote Sensing of Environment* 114, no. 12 (Dec 15 2010): 2841-52.

Kashian, D. M., and J. A. Witter. "Assessing the Potential for Ash Canopy Tree Replacement Via Current Regeneration Following Emerald Ash Borer-Caused Mortality on Southeastern Michigan Landscapes." [In English]. *Forest Ecology and Management* 261, no. 3 (Feb 2011): 480-88.

Key, T., T. A. Warner, J. B. McGraw, and M. A. Fajvan. "A Comparison of Multispectral and Multitemporal Information in High Spatial Resolution Imagery for Classification of Individual Tree Species in a Temperate Hardwood Forest." [In English]. *Remote Sensing of Environment* 75, no. 1 (Jan 2001): 100-12.

Kovacs, K. F., R. G. Haight, D. G. McCullough, R. J. Mercader, N. W. Siegert, and A. M. Liebhold. "Cost of Potential Emerald Ash Borer Damage in Us Communities, 2009-2019." [In English]. *Ecological Economics* 69, no. 3 (Jan 2010): 569-78.

Kreutzweiser, David, Dean Thompson, Susana Grimalt, Derek Chartrand, Kevin Good, and Taylor Scarr. "Environmental Safety to Decomposer Invertebrates of Azadirachtin (Neem) as a Systemic Insecticide in Trees to Control Emerald Ash Borer." *Ecotoxicology and Environmental Safety* 74, no. 6 (Sep 2011): 1734-41.

Latif, Zulkiflee Abd. "Determination of Tree Species Using Worldview-2 Data." Paper presented at the 2012 IEEE 8th International Colloquium on Signal Processing and its Applications, 2012.

Liu, X. H., Y. Sun, and Y. Wu. "Reduction of Hyperspectral Dimensions and Construction of Discriminating Models for Identifying Wetland Plant Species." [In Chinese]. *Spectroscopy and Spectral Analysis* 32, no. 2 (Feb 2012): 459-64.

Lu, D., M. Batistella, E. Moran, and E. E. de Miranda. "A Comparative Study of Landsat Tm and Spot Hrg Images for Vegetation Classification in the Brazilian Amazon." [In English]. *Photogrammetric Engineering and Remote Sensing* 74, no. 3 (Mar 2008): 311-21.

McKenzie, Nicole, Blair Helson, Dean Thompson, Gard Otis, John McFarlane, Teresa Buscarini, and Joe Meating. "Azadirachtin: An Effective Systemic Insecticide for Control of Agrilus Planipennis (Coleoptera: Buprestidae)." *Journal of Economic Entomology* 103, no. 3 (Jun 2010): 708-17.

McLaren, D., D. R. Thompson, A. G. Davies, M. T. Gudmundsson, and S. V. Chien. "Automatic Estimation of Volcanic Ash Plume Height Using Worldview-2 Imagery." Paper presented at the Annual Conference on Algorithms and Technologies for Multispectral, Hyperspectral, and Ultraspectral Imagery XVIII, Baltimore, MD, Apr 23-27 2012.

Myung, I. J. "Tutorial on Maximum Likelihood Estimation." [In English]. *Journal of Mathematical Psychology* 47, no. 1 (Feb 2003): 90-100.

Neuenschwander, A. L., L. A. Magruder, and M. Tyler. "Landcover Classification of Small-Footprint, Full-Waveform Lidar Data." [In English]. *Journal of Applied Remote Sensing* 3 (Aug 2009): 13.

Petrides, George A. "A Field Guide to Eastern Trees (Peterson Field Guides)." edited by Janet Wehr. Boston: Houghton Mifflin, 1988.

Petritan, A. M., B. von Lupke, and I. C. Petritan. "Influence of Light Availability on Growth, Leaf Morphology and Plant Architecture of Beech (Fagus Sylvatica L.), Maple (Acer Pseudoplatanus L.) and Ash (Fraxinus Excelsior L.) Saplings." [In English]. *European Journal of Forest Research* 128, no. 1 (Jan 2009): 61-74.

Pimentel, D., R. Zuniga, and D. Morrison. "Update on the Environmental and Economic Costs Associated with Alien-Invasive Species in the United States." [In English]. *Ecological Economics* 52, no. 3 (Feb 2005): 273-88.

Richardson, D. M., R. M. Cowling, and D. C. Lemaitre. "Assessing the Risk of Invasive Success in Pinus and Banksia in South-African Mountain Fynbos." [In English]. *Journal of Vegetation Science* 1, no. 5 (Dec 1990): 629-42.

Ruesink, Jennifer L., Ingrid M. Parker, Martha J. Groom, and Peter M. Kareiva. "Reducing the Risks of Nonindigenous Species Introductions." *BioScience* 45, no. 7 (1995): 465-77.

Rundquist, D. C., L. H. Han, J. F. Schalles, and J. S. Peake. "Remote Measurement of Algal Chlorophyll in Surface Waters: The Case for the First Derivative of Reflectance near 690 Nm." *Photogrammetric Engineering and Remote Sensing* 62, no. 2 (Feb 1996): 195-200.

SanMiguelAyanz, J., and G. S. Biging. "Comparison of Single-Stage and Multi-Stage Classification Approaches for Cover Type Mapping with Tm and Spot Data." [In English]. *Remote Sensing of Environment* 59, no. 1 (Jan 1997): 92-104.

Schubert, Elizabeth. "Ash Borer Invades Monroe County." Rochester: 13WHAM, 2010.

Sepulcre-Canto, G., P. J. Zarco-Tejada, J. C. Jimenez-Munoz, J. A. Sobrino, E. de Miguel, and F. J. Villalobos. "Detection of Water Stress in an Olive Orchard with Thermal Remote Sensing Imagery." *Agricultural and Forest Meteorology* 136, no. 1-2 (Jan 2006): 31-44.

Singh, N., and N. F. Glenn. "Multitemporal Spectral Analysis for Cheatgrass (Bromus Tectorum) Classification." [In English]. *International Journal of Remote Sensing* 30, no. 13 (2009): 3441-62.

Taylor, R. A. J., L. S. Bauer, T. M. Poland, and K. N. Windell. "Flight Performance of Agrilus Planipennis (Coleoptera: Buprestidae) on a Flight Mill and in Free Flight." [In English]. *Journal of Insect Behavior* 23, no. 2 (Mar 2010): 128-48.

Townsend, P. A., and S. J. Walsh. "Remote Sensing of Forested Wetlands: Application of Multitemporal and Multispectral Satellite Imagery to Determine Plant Community Composition and Structure in Southeastern Usa." [In English]. *Plant Ecology* 157, no. 2 (Dec 2001): 129-49A.

Tso, B., and P. M. Mather. "Crop Discrimination Using Multi-Temporal Sar Imagery." [In English]. *International Journal of Remote Sensing* 20, no. 12 (Aug 1999): 2443-60.

Ulyshen, M. D., R. W. Mankin, Y. G. Chen, J. J. Duan, T. M. Poland, and L. S. Bauer. "Role of Emerald Ash Borer (Coleoptera: Buprestidae) Larval Vibrations in Host-Quality Assessment by Tetrastichus Planipennisi (Hymenoptera: Eulophidae)." [In English]. *Journal of Economic Entomology* 104, no. 1 (Feb 2011): 81-86.

Wang, X. Y., Z. Q. Yang, J. R. Gould, H. Wu, and J. H. Ma. "Host-Seeking Behavior and Parasitism by Spathius Agrili Yang (Hymenoptera: Braconidae), a Parasitoid of the Emerald Ash Borer." [In English]. *Biological Control* 52, no. 1 (Jan 2010): 24-29.

Wang, X. Y., Z. Q. Yang, J. R. Gould, Y. N. Zhang, G. J. Liu, and E. S. Liu. "The Biology and Ecology of the Emerald Ash Borer, Agrilus Planipennis, in China." [In English]. *Journal of Insect Science* 10 (Aug 2010): 23.

Wolter, P. T., D. J. Mladenoff, G. E. Host, and T. R. Crow. "Improved Forest Classification in the Northern Lake-States Using Multitemporal Landsat Imagery." [In English]. *Photogrammetric Engineering and Remote Sensing* 61, no. 9 (Sep 1995): 1129-43.

Yang, Chenghai, and James H. Everitt. "Mapping Three Invasive Weeds Using Airborne Hyperspectral Imagery." *Ecological Informatics* 5, no. 5 (Sep 2010): 429-39.